ECE513 - Vector Space Signal Processing - Project Final Report: Reducing Spatially Varying Out-of-Focus Blur

Berk Iskender, berki2*
* School of Electrical and Computer Engineering, University of Illinois Urbana-Champaign, Urbana-Champaign, Illinois 61801

***Abstract*—This project final report for ECE513 - Vector Space Signal Processing includes the detailed description of the spatially varying out-of-focus blur problem, detailed critical investigation of the chosen main paper, and obtained experimental results regarding the content of the project.**

I. Introduction

Almost all digital images suffer from a common distortion which is blur. Causes of blur can be listed as out-of-focus, shake, motion etc [12]. Focus of the main paper of this project and the project itself is out-of-focus blur. Often times, when a real image is recorded by a camera, some part of the pixels are in focus but others are not. Out-of-focus blur caused by the existence of several trade-offs between aperture-size, depth-of-field and exposure time while acquiring images. A longer exposure time allow sensors to capture sufficient light but it may lead to a motion-blurred image. On the other hand, utilizing a larger aperture can prevent the motion-blur but it causes out-of-focus blur and limited depth-of-field. [39] Thinking pixel-wise, out-of-focus blur is caused by a pixel capturing additional light form its surrounding pixels and it is characterized by a point spread function (PSF) or kernel. Currently, many methods assume that blur is uniform on the whole image, meaning that the measurement is a noisy version of the original image convolved with a single blurring kernel. However, blur generally varies over the image plane and this type of blur is called as spatially-variant.

Removal of this type of blur has two main challenges:

1) It constitutes a blind deconvolution problem since both blur kernel and the convolved true image is unknown.
2) Resulting problem is fairly complex since blur kernel differs from pixel to pixel and it prevents us to use a circulant matrix to deconvolve. Because of this, many existing methods segment the blurred image into regions and use a uniform kernel for each region. (segmentation-based-deblurring methods) However, majority of natural images can not be segmented reasonably.

In the rest of the report, main paper is discussed in the perspective of the course content of ECE513. Major critics, additions and explanations are marked with bold font to indicate their places.

Important note: In the following parts, work done by the authors of the main paper [1] is investigated. Corrections and further explanations regarding proofs and links to course content is highlighted where necessary after or before the proofs and propositions. Also, connections to the lecture notes are highlighted by bold font and **LECTURE NOTES** title. Also, results related to own implementation is included at the end of the paper.

II. Blur Map Estimation and Kernel Matrix construction

The kernel or PSF of out-of-focus blur is usually approximated by a 2D Gaussian distribution function, denoted as "$g(\mathbf{x}, \sigma(\mathbf{x}))$". In this formulation, standard deviation $\sigma(\mathbf{x})$, measures the amount of blur on the pixel $\mathbf{x} = (x, y)$, where the pair (x, y) is the 2D coordinates of the corresponding pixel. Thus, a reasonable approach is to predict $\sigma(\mathbf{x})$ first and utilize it to generate kernel $g(\mathbf{x}, \sigma(\mathbf{x}))$. Then, removing the blur using $g(\mathbf{x}, \sigma(\mathbf{x})) \in \mathbb{R}^{MxN}$, which is the same size of the deblurred image. $\sigma(\mathbf{x})$ is generally called as "blur map".

Therefore, we can formulate our system as follows:

$$b(x) = (g \circledast f)(x) + n(x) = \int_{\Omega} g(y) f(x - y) dy + n(x) \quad (1)$$

where $b : \Omega \to \mathbb{R}$ is the blurred image of size M x N, modeled as the convolution of its clear version f at every pixel $\mathbf{x}$, $\circledast$ is the convolution operator, $\mathbf{n}$ is the additive noise. Only b is given in this equation which makes (1) an underconstrained problem, where number of unknown variables exceeds the number of equations. Additional assumptions are needed to obtain sufficient results.

A. Blur Map Estimation

Usually, blurred image is smoother than the original version of the image due to the nature of blur on digital images. This means as image gets more blurry, average difference between pixel values of the image decreases. This motivates the idea of using a variable describing the overall difference in w_x to quantify the amount of blur on $\mathbf{x}$, where w_x is a neigborhood of the pixel $\mathbf{x}$.

Additional information (Holder's Coefficient, Holder Spaces): Authors of the paper suggest that Holder's coefficient satisfies this requirement without giving any additional information on the topic of Holder's coefficient. Thus, it is fairly helpful to provide some information related to this topic before going further with the project.

Holder's Condition and Holder's Coefficient: A real or complex-valued function satisfies is Holder continuous, if there exist nonnegative real constants $C, \alpha > 0$ such that

$$|f(x) - f(y)| \leq C||x - y||^{\alpha} \quad (2)$$

$\forall x, y \in dom(f)$. The number α is called the exponent of the Holder condition. If the function satisfies the condition with $\alpha > 1$ it is a constant function. If $\alpha = 1$, the function satisfies a Lipschitz condition. For any $\alpha > 0$, the condition implies the function is uniformly continuous.

Holder Spaces: Holder space is a $C^{k,\alpha}(\Omega)$ where Ω is an open some Euclidean space and $k \geq 0$ is an integer, representing that those functions on Ω having

1) continuous derivatives up to order k
2) such that kth partial derivatives are Holder continuous with exponent α, where $0 < \alpha \leq 1$.

Holder spaces are vector spaces since they satisfy the vector addition and scalar multiplication and remaining 8 axioms: Associavity, commutativity, identity element, distributivity etc. Assuming $f, g \in C^{k,\alpha}(\Omega)$ (meaning that they satisfy both conditions listed above), then, $f + g \in C^{k,\alpha}(\Omega)$ and $\beta f, \beta g \in C^{k,\alpha}(\Omega)$ holds.

LECTURE NOTES - Chapter 4 - Linear Vector Spaces:

A linear vector space is a set X along with a field of scalars F, and two operations $+ : X \times X \to X$ and $. : F \times X \to X$ s.t.

1. $a + b = b + a$ for $a, b \in \mathcal{X}$.
2. $(a + b) + c = a + (b + c)$ for $a, b, c \in \mathcal{X}$.
3. $0 \in \mathcal{X}$ such that $a + 0 = a$ for every $a \in \mathcal{X}$.
4. $\alpha \cdot (\beta \cdot \mathcal{X}) = (\alpha\beta) \cdot \mathcal{X}$
5. $\alpha \cdot (b + c) = \alpha \cdot b + \alpha \cdot c$
6. $(\alpha + \beta) \cdot \boldsymbol{a} = \alpha \cdot \boldsymbol{a} + \beta \cdot \boldsymbol{a}$
7. $0 \cdot \boldsymbol{a} = \mathbf{0}, 1 \cdot \boldsymbol{a} = \boldsymbol{a}$

Furthermore, **Holder coefficient** where k = 0,

$$|f|_{C^{k,\alpha}(\Omega)} = \sup_{x \neq y \in \Omega} \frac{f(x) - f(y)}{||x - y||^{\alpha}} \tag{3}$$

is finite, the function is Holder continuous and coefficient serves as a **seminorm**. It satisfies all of the properties of a norm except that it can be 0 without $[b]^{\beta}_{w_x}$

LECTURE NOTES - Chapter 4 - Norm / Seminorm: A norm is a real-valued functional on a LVS X, $||.|| : X \to \mathbb{R}$, that satisfies:

1) $\|\boldsymbol{x}\| \geq 0$ for all $\boldsymbol{x} \in \mathcal{X}$, with equality if and only if $\boldsymbol{x} = 0$
2) $\|x + z\| \leq \|x\| + \|z\|$ for all $x, z \in \mathcal{X}$
3) $\|\alpha \boldsymbol{x}\| = |\alpha| \|\boldsymbol{x}\|$ for all $\boldsymbol{x} \in \mathcal{X}, \alpha \in \mathbb{F}$

Likewise, semi-norm is defined as a relaxed version of norm: **Additional information - Seminorm:** A seminorm is a functional on a LVS X, $||.|| : X \to \mathbb{R}$, that satisfies:

1) $\|x\| \geq 0$ ($||x|| = 0$ can be satisfied without $x = 0$)
2) $\|cx\| = |c| \|x\|$, and
3) $\|x + y\| \leq \|x\| + \|y\|$, $\forall x, y \in X$ and $c \in \mathbb{F}$

As a regularity, the Holder coefficient has been applied to many image processing tasks. In the context of the paper, Holder's coefficient is defined as:

$$[b]^{\beta}_{w_x} = \sup_{y,z \in w_x,\ y \neq z} \{ \frac{|b(y) - b(z)|}{||y - z||^{\beta}} \} \tag{4}$$

where $\beta \geq 0$ is a parameter. If it is taken as 0, we obtain

$$[b]^{0}_{w_x} = \max_{y \in w_x} \{b(y)\} - \min_{y \in w_x} \{b(y)\} \tag{5}$$

Then, we can treat $\frac{[b]^{\beta}_{w_x}}{[b]^{0}_{w_x}}$ as the normalized Holder coefficient (NHC). For practical purposes, authors take $|w_x| = 7x7$ and $\beta = 2$.

Empirically, it is observed that NHC varies almost inversely to the level of the blur. For practical purposes, authors treated this relation as a linear correlation.

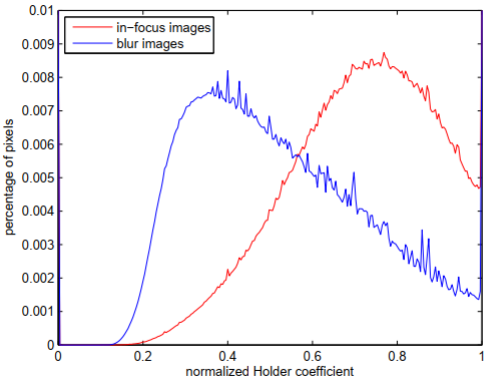

Fig. 1: The distributions of the NHC for in-focus (red) and blur images (blue). [1]

Authors provided the empirical results related to the distributions of the NHC for in-focus and out-of-focus blur images using 1000 natural blurry and 1000 natural in-focus images.

Then, an initial version of blur map $\tilde{\sigma(\mathbf{x})}$ is obtained as

$$\tilde{\sigma(\mathbf{x})} = \frac{C}{\frac{[b]^{\beta}_{w_x}}{[b]^{0}_{w_x}}} = C \frac{[b]^{0}_{w_x}}{[b]^{\beta}_{w_x}} \tag{6}$$

where C is a constant parameter. This initial version of blur map has excessive sharp transitions due to edges and noise. This causes a need for refinement. Blur map refinement problem can be defined as follows:

$$\nu ||\nabla \sigma|| + ||\Pi \odot (\sigma - \tilde{\sigma})||^2 \tag{7}$$

where $\sigma > 0$ is a balanced parameter, ∇ is gradient operator and $\odot$ is the Hadamard product. Π is an edge indicator function,

$$\Pi(\boldsymbol{x}) = \begin{cases} 1, & \|\nabla \mathbf{b}(\boldsymbol{x})\| > \xi \\ 0, & \text{otherwise} \end{cases}$$

where $\xi > 0$ is a parameter. Respective problem $E(\sigma)$ can be solved using Chambolle-Pock algorithm [2]:

1) $p^{n+\frac{1}{2}} = p^n + \tau \lambda \nabla \sigma^n$
2) $p^{n+1} = \frac{p^{n+\frac{1}{2}}}{\max(1, |p^{n+\frac{1}{2}}|)}$
3) $\sigma^{n+1} = \frac{\Pi \odot \tilde{\sigma} + \sigma^n}{\gamma \Pi + 1}$

where τ and γ are positive parameters.

Fig. 2: A spatially-varying blurred image

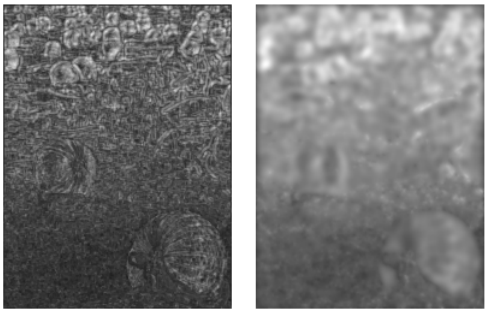

(a) (b)

Fig. 3: The blur maps of Figure 2 (800 600 pixels): (a) the rough blur map $\tilde{\sigma}$; (b) the refined blur map σ. [1]

B. Kernel Matrix Analysis:

Having blur map computed, blur kernel $g(\mathbf{x}, \sigma(\mathbf{x}))$ can be computed. However, solution for (1) is has a very high time complexity since σ is different for every pixel, (1) should be solved pixel-by-pixel. Thus, a reformulation of the corresponding problem is used:

$$b = Af + n \tag{8}$$

where b, f, n are the vectorized of corresponding 2D image counterparts in (1) of size M x N. Kernel matrix A (size MN x MN) is the matrix form of the kernel $g(\mathbf{x}, \sigma(\mathbf{x}))$. Different than the spatially-invariant matrices, rows of spatially-variant matrix A can have different variances. Furthermore, there are additional properties that the matrix A satisfies.

Proposition 1. (Error Correction: The original version of this proposition takes A into account instead of A^TA. However, as I will show in the proof, in order to use A, we need an additional symmetry property which does not necessarily hold for the matrix A. Thus, a corrected version is provided.) Let λ_m be the largest eigenvalue of A^TA, then the $\lambda_m \leq 1$ holds.

Additional Proof: Proof for this proposition requires the utilization of Gershgorin's Circle Theorem. However, authors used the result of this theorem without proving it. Thus, I provide the proof of this theorem.

LECTURE HW2 - Gershgorin's Circle Theorem: Let $R_j(A) = \sum_{j \neq i} |a_{ji}|$ and $D(a_{ii}, R_i) \subseteq C$ be a closed disc centered at $A_i i$ with radius R_i. Such a disc is called a Gershgorin disc. Theorem states that every eigenvalue of A lies in at least one of D's.

Proof: Let (x, λ) be an eigenpair of A where $x_i = 1$ and $|x_j| \leq 1$ for $j \neq i$. In particular: $Ax = \lambda x$ can be written. Then,

$$\sum_j a_{ij} x_j = \lambda x_i = \lambda . 1 = \lambda$$

Thus, $\sum_{j \neq i} a_{ij} x_j + a_{ii} x_i = \sum_{j \neq i} a_{ij} x_j + a_i i = \lambda$. Applying triangular inequality, we obtain:

$$|\lambda - a_i i| = |\sum_{j \neq i} a_{ij} x_j| \leq \sum_{j \neq i} |a_{ij}||x_j| \leq \sum_{j \neq i} |a_{ij}| = R_i$$

■

Now, we can apply this theorem to prove the proposed claim.

Proof of Proposition 1 (cntd.): By Gershgorin's Circle Theorem, all eigenvalues of $B = A^TA$ are located in the union of MN discs, centered at B_{jj}'s. We can express this union as:

$$\cup_{j=1}^{MN} \{|z - B_{jj}| \leq R_j(B)\} = G(B)$$

$G(B) \subset U$, U being the unit disc centered at origin. This can be further shown as:

$$R_j(B) \leq R_j(B) + |B_{jj}| = \sum_{k=1}^{MN} |B_{jk}| = 1$$

Following the definition provided at the beginning of the proof for Gershgorin's Circle Theorem, sum of $R_j(B)$ (radius of the disc) and B_{jj} (center) does not exceed 1 for any of the MN circles. This guarantees that every such circle should stay inside the unit circle. Thus, all eigenvalues are smaller than the radius of U, i.e. $\lambda_m \leq 1$.

Proposition 2. Let $\mathbf{x} = (x_1, x_2)$, $\mathbf{y} = (y_1, y_2)$ and let $diag(\sigma)$ be the corresponding diagonal matrix, and A^i be the matrix form of 1-D Gaussian kernel g^i toward i-axis,

$$g^i(\mathbf{x})(y_i) = \frac{1}{\sqrt{2\pi}\sigma(\mathbf{x})} exp(\frac{-|y_i - x_i|^2}{2\sigma^2(\mathbf{x})}), \;\; i = 1, 2$$

Then, we have

$$A = \sqrt{2\pi} diag(\sigma) A^1 A^2$$

Proof: We know that $g(\mathbf{x}, \sigma(\mathbf{x}))$ is a 2D Gaussian distribution function.

$$g(\mathbf{x}, \sigma(\mathbf{x}))(\mathbf{y}) = \frac{1}{\sqrt{2\pi\sigma(\mathbf{x})}} exp(\frac{-||\mathbf{y} - \mathbf{x}||^2}{2\sigma^2(\mathbf{x})})$$

for $y \in N_x$, where N_x is a specified neighborhood of $\mathbf{x}$.
Using the separability of Gaussian fct. this can be rewritten as:

$$\begin{aligned} g(\mathbf{x}, \sigma(\mathbf{x}))(\mathbf{y}) &= \frac{1}{\sqrt{2\pi\sigma(\mathbf{x})}} exp(\frac{-|y_1 - x_1|^2}{2\sigma^2(\mathbf{x})}) exp(\frac{-|y_2 - x_2|^2}{2\sigma^2(\mathbf{x})}) \\ &= \sqrt{2\pi}\sigma(\mathbf{x}) g^1(\mathbf{x})(y_1) g^2(\mathbf{x})(y_2) \end{aligned}$$

Then, $(g \circledast f)(\mathbf{x}) = \sqrt{2\pi}\sigma(\mathbf{x}) g^1(\mathbf{x}) \circledast g^2(\mathbf{x}) \circledast f(\mathbf{x})$. Matrix formulation of the respective formula can be written for the complete image as:

$$\sqrt{2\pi} diag(\sigma) A^1 A^2.$$

■

For the remaining proofs of propositions, we need to declare the induced norm for matrix A as

$$||A|| = \max\{||A\Phi|| : ||\Phi|| \leq 1\}$$

Proposition 3.: Let σ_m be the largest value in $|\sigma|$ the norm of the kernel A is bounded by $||A|| \leq L$ where $L = \sqrt{2\pi}(\frac{\pi^2}{2} - 2)\sigma_m$.

Additional Proof: Before proving this proposition, we need to prove the CS inequality. Authors used the result without showing the correctness of it. Thus, I add the corresponding proof.

LECTURE NOTES - Chapter 4 - Cauchy-Schwarz Inequality: For every $x, y \in X$,

$$| < x, y > | \leq \sqrt{< x, x >} \sqrt{< y, y >}$$

with equality if and only if $y = 0$ or $x = \alpha y$, $\alpha \in F$.

Proof: The result is obvious for $y = 0$. For $y \neq 0$, by the positivity of the inner product,

$$0 \leq < x - \alpha y, x - \alpha y > =$$

$$< x, x > + |\alpha|^2 < y, y > - \alpha < y, x > + \overline{\alpha} < x, y >$$

Taking $\alpha = \frac{\langle x,y \rangle}{\langle y,y \rangle}$, expression simplifies to

$$0 \leq < x, x > - \frac{| < x, y > |^2}{< y, y >}$$

which leads to the inequality. ∎

Proof of Proposition 3 (cntd.): Using Property 2.2, following result using Cauchy-Schwarz inequality, knowing that it can be generalized for more than to elements:

$$||A|| = \sqrt{2\pi} ||A^1|| \, ||A^2|| \, ||diag(\sigma_m)|| \tag{9}$$

Also, we know that the induced norm of the $diag(\sigma)$ is its largest singular value:

$$||diag(\sigma)|| = \sigma_m$$

LECTURE NOTES - Chapter 2 - Thm 2.5: Let $W = U\Sigma V^*$ be the SVD decomposition of the framelet transform matrix W. We can show that the induced norm of W is equal to its largest singular value. Thm 2.5 states that:

$$||W|| = \max_{||x||_2=1 \ , \ x \perp v_1, \ldots, v_k} ||Wx||_2^2 = \sigma_{k+1}^2 \ , \ \ k = 0, \ldots, n$$

$$\implies \max_{||x||_2=1} ||Wx||_2^2 = ||W||_2 = \sigma_1^2 \ \ if \ \ k = 0$$

where $||W||_2 = ||W||$ is the induced norm of the matrix W.

Proof: Let $z = \tilde{V}^* x$. Then, $||z||_2^2 = x^* \tilde{V} \tilde{V}^* x = ||x||_2^2$. Thus,

$$\max_{||x||_2=1 \ , \ x \perp v_1, \ldots, v_k} ||Wx||_2^2 = \max_{||z||_2=1 \ , \ z_1 = \ldots = z_k = 0} ||W\tilde{V}z||_2^2$$

$$= \max_{||z||_2=1 \ , \ z_1 = \ldots = z_k = 0} ||\tilde{U}\tilde{\Sigma}z||_2^2$$

∎

Proof of Proposition 3 (cntd.): To obtain bound of $||A^1||$, we can look at bound of $||A^1\Phi||^2$, where Φ is as stated in the induced norm definition.

$$||A^1\Phi||^2 = \sum_{j=1}^{MN} (\sum_{k=1}^{MN} A_{jk}^1 \Phi_k)^2 \leq 2 \sum_{j=1}^{MN} \sum_{k=1}^{MN} (A_{jk}^1)^2 (\Phi_k)^2$$

$$= 2 \sum_{j=1}^{MN} (\sum_{k=1}^{MN} (A_{jk}^1)^2) \Phi_k^2 \tag{10}$$

where A^1 is the matrix form of g^1. The inequality follows as a generalization of $a^2 + b^2 \geq 2ab$ which is not stated in the paper. Let $j = (x_2 - 1)M + x_1$. Then, jth row of A^1 is exactly constructed from the discrete version of $g^1(x)$. Given g^1 with arbitrary variance, following inequality holds:

$$g^1(\mathbf{x})(y_1) < \frac{1}{2k+1} \tag{11}$$

when $|y_1 - x_1| = k$. Reason of why this inequality holds is not explicitly stated in the paper. Therefore, I will provide the explanation. Since image plane is a discrete 2D plane and respective g^1 and g^2 are discrete 1D Gaussian distribution functions, for instance, if $|y_1 - x_1| = k$, meaning that point of interest y_1 is k pixels away from the mean point $|x_1|$. Since any Gaussian function has its peak at its mean and sum of its all elements is 1, if $g^1(\mathbf{x})(y_1) \leq \frac{1}{2k+1}$, rest of the closer elements should exceed this value and sum exceeds 1. Thus, (11) should hold. Following this, since A^1 is the matrix form of g_1, upper bound of A_{ij}^1 is given by the following equation as a generalization:

$$A_{jk}^1 < \frac{1}{2|j-k|+1}$$

where $j, k \in [1, MN]$. Then, (10) can be rewritten as:

$$||A^1\Phi||^2 \leq 2 \sum_{k=1}^{MN} \Phi_k^2 \sum_{j=1}^{MN} (\frac{1}{2|j-k|+1})^2$$

$$\leq 2 \sum_{k=1}^{MN} \Phi_k^2 (2 \sum_{j=0} \frac{1}{(2j+1)^2} - 1)$$

$$\leq 2(2 \sum_{j=0} \frac{1}{(2j+1)^2} - 1) = 2(\frac{3}{2} \sum_{j=1} \frac{1}{j^2} - 1) = \frac{\pi^2}{2} - 2$$

$$\implies ||A^1|| < \sqrt{\frac{\pi^2}{2} - 2}$$

Also, g^2 is the same as g^1 but it is in the other direction, meaning that the bound for $||A^2||$ is the same as $||A^1||$.

Combining the results and plugging them into (9), we obtain:

$$||A|| \leq \sqrt{2\pi} ||diag(\sigma)|| \, ||A^1|| \, ||A^2|| \leq \sqrt{2\pi} (\frac{\pi^2}{2} - 2) \sigma_m = L$$

Sparse Kernel Matrix Analysis: Theoretically, $g(\mathbf{x}, \sigma(\mathbf{x}))$ will be nonzero at every point of the image, thus, N_x should be the entire image. However, in practice, pixels at a distance $k \geq 3\sigma(\mathbf{x})$ can be considered as 0 with no contributions to the measurements since g is a Gaussian distribution function with mean **x** and standard deviation $\sigma(\mathbf{x})$.

This suggest that radius of the neighborhood N_x can be taken as $r_x = 3\sigma(\mathbf{x})$ is set for convolution processes.

A becomes sparse, each column/row having at most $(2r+1)^2$ non-zero elements where $r = max\{r_x\}$ is the determined by the largest standard deviation that Gaussian distributions on each pixel has. $(2r+1)^2$ is the approximate number of nonzero elements because the region that is selected as the neighborhood is a square region having one edge of length $(2r+1)$.

In accordance with the respective claim, following proposition can be suggested:

Proposition 4: The norm of the sparse kernel matrix A is bounded by $||A|| < (2r+1)^2$.

Additional Proof: Proof of this theorem is not stated in the paper itself. They referred to another paper for the result that they readily use for their purposes. Thus, starting form the given reference, I provide the proof completely.

For the upper bound of the eigenvalues of the matrix $A^\dagger A$, I will refer to Theorem 2.1. in [3]:

Theorem: Assuming that $c_{aj}(A) = \sum_{i=1}^{I} |A_{ij}|^{2-a}$ and $r_{ai}(A) = \sum_{j=1}^{J} |A_{ij}|^{2-a}$ for any a in the interval [0,2], no eigenvalue of the matrix $A^\dagger A$ exceeds the maximum of

$$\sum_{j=1}^{J} c_{aj} |A_{ij}|^{2-a}$$

over all i, nor the maximum of

$$\sum_{i=1}^{I} r_{ai}|A_{ij}|^a$$

over all j. Thus, no eigenvalue of $A^\dagger A$ exceeds $c_a r_a$.

Proof of the theorem: Let $A^\dagger Av = \lambda v$ and $w = Av$. Then,

$$||A^\dagger w||^2 = \lambda ||w||^2$$

can be written. Utilizing Cauchy-Schwarz inequality (as shown previous in the proof of Proposition 2.3): (**LECTURE NOTES - Chapter 4 - Thm 4.6**)

$$|\sum_{i=1}^{I} \bar{A}_{ij} w_i|^2 \leq (\sum_{i=1}^{I} |A_{ij}|^{\frac{a}{2}} |A_{ij}|^{1-\frac{a}{2}} |w_i|)^2$$

$$\leq (\sum_{i=1}^{I} |A_{ij}|^a)(\sum_{i=1}^{I} |A_{ij}|^{2-a}|w_i|^2)$$

Following this result, we can write

$$||A^\dagger w||^2 \leq \sum_{j=1}^{J}(c_{aj}(\sum_{i=1}^{I} |A_{ij}|^{2-a}|w_i|^2)) = \sum_{i=1}^{I}(\sum_{j=1}^{J} c_{aj}|A_{ij}|^{2-a})|w_i|^2$$

$$\leq \max_i(\sum_{j=1}^{J} c_{aj}|A_{ij}|^{2-a})||w||^2$$

As given at the beginning of the proof, expressions $\sum_{j=1}^{J} c_{aj}|A_{ij}|^{2-a}$ and $\sum_{i=1}^{I} r_{ai}|A_{ij}|^a$ are same and obtained upper bound can also be expressed as

$$\leq \max_j(\sum_{i=1}^{I} r_{ai}|A_{ij}|^a)||w||^2$$

which concludes the proof of Theorem 2.1 in [3].

Then, using the result of this proof, we can show that Proposition 2.4 holds true. Utilizing the result, we can state that all singular values of A, σ_i , $i \in \{1, ..., MN\}$ satisfies the following inequality:

$$\sigma_i \leq \max_k\{\sum_{j=1}^{MN} |A_{jk}|^\alpha\}.\max_j\{\sum_{k=1}^{MN} |A_{jk}|^{2-\alpha}\}$$

Letting $\alpha = 1$, since $\sum_{k=1}^{MN} |A_{jk}| = 1$ and each column has at most $(2r+1)^2$ nonzero elements, we have:

$$||A|| \leq \max_k\{\sum_{j=1}^{MN} |A_{jk}|\} \max_j\{\sum_{k=1}^{MN} |A_{jk}|\} \leq \max_k\{\sum_{j=1}^{MN} |A_{jk}|\} \leq (2r+1)^2$$

since $\max_j\{\sum_{k=1}^{MN} |A_{jk}|\} \leq 1$.

III. Deblurring formulation based on framelet system:

In the paper, authors provided brief introduction to the framelet system in univariate setting. Fortunately, for bivariate settings, tensor product can be used to generalize obtained results.

A. Framelets and image representation:

Firstly, we should define the term "tight frame". A countable function subset $X \subset L^2(\mathbb{R})$ is called a tight frame of $L^2(\mathbb{R})$ if $\forall f \in L^2(\mathbb{R})$

$$f = \sum_{h \in X} \langle f, h\rangle h \tag{12}$$

or equivalently,

$$||f||^2 = \sum_{h \in X} |\langle f, h\rangle|^2, \forall f \in L^2(\mathbb{R})$$

LECTURE NOTES - Chapter 4 - Induced Norms on IPS - The L_2 IPS: $\langle f, g\rangle = \int_{t \in R} f(t)g(t)dt$ is the inner product on the respective inner product space (IPS), $L^2(\mathbb{R})$ and $||.|| = \sqrt{\langle f, g\rangle}$ is a valid norm and it is the respective induced norm.

Given a finite set $\Phi = \{\phi^1, ..., \phi^r\} \subset L^2(\mathbb{R})$, a wavelet system is defined as collection of shifts and dilations of the elements of set Φ:

$$X(\Phi) = \{2^{\frac{1}{2}}\phi^j(2^k x - l) : 1 \leq j \leq r\,;\, k, l \in \mathbb{Z}\}$$

when $X(\Phi)$ forms a tight frame it is called as a wavelet tight frame and ϕ^j is a (tight) framelet. Any orthogonal basis in $L^2(\mathbb{R})$ is a tight frame since every element in $L^2(\mathbb{R})$ can be represented as in (12) using an orthogonal basis.

LECTURE NOTES - Chapter 4 - Orthogonality: In an IPS such as $L^2(\mathbb{R})$ orthogonality is defined as

$$\langle x, y\rangle = 0 \ , \ x, y \in X$$

denoted as $x \perp y$. A subset of $L^2(\mathbb{R})$ is an orthogonal set if

$$\forall x, y, \in L^2(\mathbb{R}), \ x \neq y \implies x \perp y$$

LECTURE NOTES - Chapter 4 - Hammel Basis and span: A linearly independent subset S of $L^2(\mathbb{R})$ which is an IPS and a LVS, is a Hammel basis if $Span\{S\} = L^2(\mathbb{R})$ where span(S) is defined as the set of all linear combinations of elements of S.

Due to the reasons explained above, a tight frame can be perceived as generalization of the orthogonal basis where elements do not have to be orthogonal to each other which brings redundancy to the set which is verified to be useful in many image processing applications such as deblurring. [8]

To construct a compactly supported wavelet tight frames $X(\Phi)$:

1) Obtain a compactly supported refinable function $\psi \in L^2(\mathbb{R})$ with refinement mask (a low pass filter) g_0 such that it satisfies the following:

$$\psi(x) = \sum_l g_0(l)\psi(2x - l)$$

2) Given ψ, the construction of a wavelet tight frame is actually to find an appropriate set of framelets $\Phi = \{\phi^1, ..., \phi^r\} \subset L^2(\mathbb{R})$ defined as:

$$\phi^j = \sum_l g_j(l)\psi(2x - l) \ , \ j = 1, \ldots, r$$

where g_j is a high pass filter.

The unitary extension principle states that the system $X(\Phi)$ constitutes a tight frame in $L^2(\mathbb{R})$ if: $g_0, \ldots, g_r$ satisfy

$$\gamma_{g_0}(w)\gamma_{g_0}(\bar{w} + \beta\pi) + \sum_{j=1}^{r} \gamma_{g_j}(w)\gamma_{g_j}(\bar{w} + \beta\pi) = \delta(\beta) \ , \ (\beta = 0, 1)$$

where $\gamma_{g0}(w) = \sum_l g(l)e^{jlw}$ and $\delta(\beta)$ is the delta function.

In the numerical scheme, framelet transform can be represented by a matrix W. Using W, frame coefficient vector u is given by

$$u = Wf$$

for a vector f. Also, frame reconstruction can be described as:

$$f = W^T u$$

where W^T is the inverse wavelet transformation. Following property is satisfied for all wavelet transforms:

$$f = W^T W f \implies W^T W = I$$

However, if the rows are not orthogonal to each other, we have $WW^T \neq I$.

For bivariate case, corresponding W can be obtained by using Kronecker product of corresponding univariate W of size MxN

$$W \otimes W = \begin{bmatrix} w_{11}W \dots w_{1N}W \\ \dots \\ w_{M1}W \dots w_{MN}W \end{bmatrix}$$

IV. Proposed optimization model

To reconstruct clear image f, we need to solve

$$\min_f R(f) + F(f)$$

where R(f) is the regularization term and F(f) is the data fidelity term.

Since images have sparse approximations in the framelet domain, this prior is used and $R(f) = ||Wf||_1$ where W is the framelet decomposition operator.

The data fidelity term F(f) determined by the noise distribution existing in the measurement i.e. for impulse noise $l_1 - norm$, for Gaussian noise $l_2 - norm$. However, in practical aspects, noise does not completely belong to a single distribution. Instead, it generally behaves like a mixture of distributions. Thus, data fidelity term is selected as $l_p - norm$ to account for the different mixtures of noises

$$F(f) = ||Af - b||_p^p$$

where $p \in [1, 2]$ is adjusted to minimize the reconstruction error in the problem above.

LECTURE NOTES - Chapter 4 - Ex. 4.23: On $C[a, b]$, for $1 \leq p < \infty$:

$$\|\boldsymbol{x}\|_p = \left[\int_a^b |x(t)|^p dt\right]^{1/p}$$

Triangle inequality for this norm is Minkowski inequality for integrals.

Then, complete optimization problem can be stated as

$$\min_f \mu||Wf||_1 + \frac{1}{p}||Af - b||_p^p, \;\; p \in [1, 2] \tag{13}$$

A. Algorithm

In this subsection, the numerical algorithm of the complete out-of-focus deblurring method will be described. Authors adapted a primal-dual algorithm for (13) since it is a convex $l_1 - norm$ minimization problem. (Since W is a linear transformation)

The saddle-point formulation of (13) can be obtained by using the fact that $l_1 - norm$ and $l_\infty - norm$ are duals of each other.

$$||Wf||_1 = \max_{||d||_\infty \leq 1} \langle Wf, d\rangle$$

Then, we can formulate the saddle point formulation as follows:

$$\min_f \max_d \mu\langle Wf, d\rangle + \frac{1}{p}||Af - b|| - \delta_D(d) \tag{14}$$

where $D = \{d : ||d||_\infty \leq 1\}$, δ_D is the indicator function as described below

$$\delta_D(d) = 0, \;\; d \in D$$

$$= \infty, \;\; , d \notin D$$

Proposition 5: Framelet transformation is linear and the induced norm of its matrix form satisfies the following property:

$$||W|| = 1$$

Proof: Since $W^T W = I$ and $||W^T|| = ||W|| \implies ||W|| = 1$

LECTURE NOTES - Contribution to proof in accordance with course content: Authors did not provide any additional information in this proof. However, using the definition of the induced norm and SVD, we can show the correctness of this proposition in a better way.

LECTURE NOTES - Chapter 2 - Thm 2.5: Let $W = U\Sigma V^*$ be the SVD decomposition of the framelet transform matrix W. We can show that the induced norm of W is equal to its largest singular value. Thm 2.5 states that:

$$||W|| = \max_{||x||_2=1 \;,\; x \perp v_1,\dots,v_k} ||Wx||_2^2 = \sigma_{k+1}^2 \;\; , \;\; k = 0, \dots, n$$

$$\implies \max_{||x||_2=1} ||Wx||_2^2 = ||W||_2 = \sigma_1^2 \;\; if \;\; k = 0$$

where $||W||_2 = ||W||$ is the induced norm of the matrix W.

Proof Thm 2.5.: Let $z = \tilde{V}^* x$. Then, $||z||_2^2 = x^* \tilde{V}\tilde{V}^* x = ||x||_2^2$. Thus,

$$\max_{||x||_2=1 \;,\; x \perp v_1,\dots,v_k} ||Wx||_2^2 = \max_{||z||_2=1 \;,\; z_1=\dots=z_k=0} ||W\tilde{V}z||_2^2$$

$$= \max_{||z||_2=1 \;,\; z_1=\dots=z_k=0} ||\tilde{U}\tilde{\Sigma}z||_2^2$$

Proof of Proposition 5 continued:
Using the fact that $||\tilde{U}x||_2^2 = x^*\tilde{U}^*\tilde{U}x = ||x||_2^2$, we obtain

$$\max_{||z||_2=1 \;,\; z_1=\dots=z_k=0} ||\tilde{U}\tilde{\Sigma}z||_2^2 = \max_{||z||_2=1 \;,\; z_1=\dots=z_k=0} ||\tilde{\Sigma}z||_2^2$$

$$\max_{||z||_2=1} \sum_{l=k+1}^{n} \sigma_l^2 z_l^2 \leq \sigma_{k+1}^2 \sum_{k=1}^{n} z_k^2 = \sigma_{k+1}^2$$

with equality if $z_{k+1} = 1$, $z_j = 0$ for $j \neq k + 1$.

Using the result of this theorem and the SVD of W,

$$U^* V \Sigma^* U^* = U\Sigma^2 U^* = I \implies \sigma_1^2 = 1$$

and

$$||W^*|| = ||V\Sigma U^*|| = ||W|| = ||U\Sigma V^*|| = \sigma_1$$

$$\implies ||W|| = 1$$

Last step is to apply a primal-dual algorithm [13] to formulation (14) since it is proper, convex and lower semi-continuous.

Regular primal-dual algorithm on (14) can be utilized as follows [2]:

1)

$$\boldsymbol{d}^{i+1} = \arg\max_{d} \mu \left\langle \mathcal{W}\boldsymbol{f}^{i+1}, \boldsymbol{d} \right\rangle - \delta_{\mathbf{D}}(\boldsymbol{d}) - \frac{1}{2\tau^i} \left\| \boldsymbol{d} - \boldsymbol{d}^i \right\|^2 \tag{15}$$

2)

$$\boldsymbol{f}^{i+1} = \arg\min_{\boldsymbol{f}} \mu \left\langle \mathcal{W}\boldsymbol{f}, \boldsymbol{d}^{i+1} \right\rangle + \frac{1}{p}\|\mathbf{A}\boldsymbol{f} - \boldsymbol{b}\|_p^p + \frac{1}{2\zeta^i} \left\| \boldsymbol{f} - \boldsymbol{f}^i \right\|^2 \tag{16}$$

3)

$$\overline{\boldsymbol{f}^{i+1}} = \boldsymbol{f}^{i+1} + \theta^i \left(\boldsymbol{f}^{i+1} - \boldsymbol{f}^i \right) \tag{17}$$

V. Results

Firstly, I will provide the synthesized experimental results and results on natural images of the main paper and secondly, I will provide the results that I obtained related to the blur map estimation and complete deblurring method.

A. Results of the main paper

Synthesized image experiments for two types of blur maps and comparisons of reconstruction with the state-of-the-art methods:

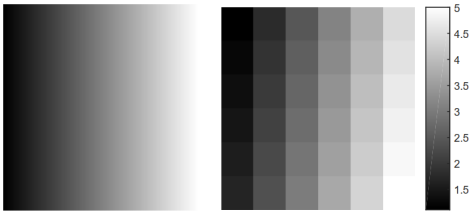

Fig. 4: The blur maps used to obtain synthesized measurements; (A): Left blur map (B): Right blur map [1]

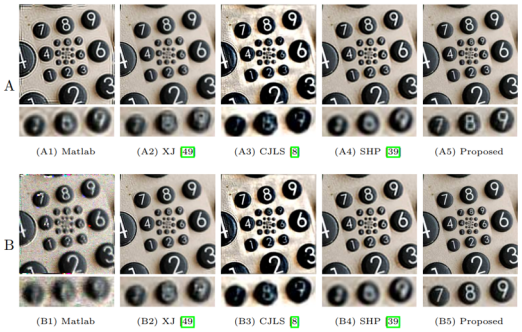

Fig. 5: Reconstruction comparisons from both blur types A and B, first image [1]

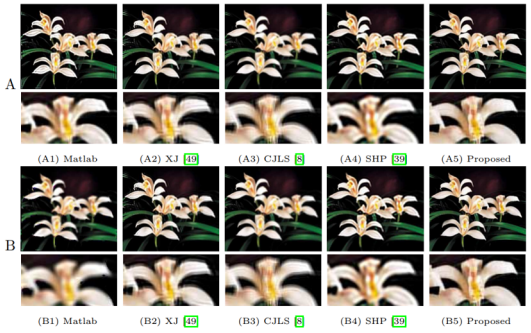

Fig. 6: Reconstruction comparisons from both blur types A and B, second image [1]

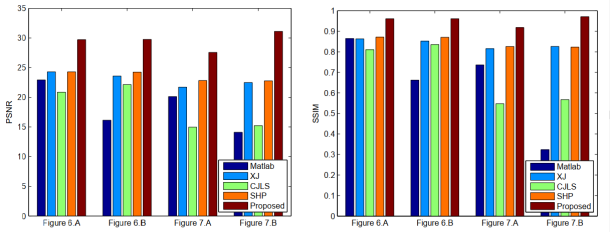

(a) PSNR (b) SSIM

Fig. 7: SSIM and PSNR comparisons of both methods for the synthesized experimental tests, NOTE: In the PSNR and SSIM pots, Figure 6 is equal to the Figure 5., Figure 7 is equal to the Figure 6. in this final report [1]

B. *Own results:*

In order to implement the method own my own, firstly, I blurred the left top quadrant of a natural image with a Gaussian kernel and applied blur map acquisition method on top of it.

After obtaining the blur map and refining it as proposed, obtained results are pretty similar to results in the main paper and we can see that the method captures most of the additional blur information on left top quadrant.

Then, I implemented the proposed optimization algorithm using stochastic gradient descent method for optimization instead of primal-dual algorithm. However, one thing to note is that my implementation is most probably fairly suboptimal since there are lots of open parameters to be optimized in the original proposed method where no information about them is shared in the paper itself. Nevertheless, my implementation of the overall method managed to deblur the image to some extent. Since I applied the method on a natural image where I did not add any additional blur, no quantitative measuring result can be provided.

References

[1] F. Fang, F. Li, and T. Zeng, "Reducing spatially varying out-of-focus blur from natural image," *Inverse Problems & Imaging*, vol. 11, no. 1, pp. 65–85, 2017.

[2] A. Chambolle and T. Pock, "A first-order primal-dual algorithm for convex problems with applications to imaging," *Journal of mathematical imaging and vision*, vol. 40, no. 1, pp. 120–145, 2011.

[3] C. Byrne *et al.*, "Bounds on the largest singular value of a matrix and the convergence of simultaneous and block-iterative algorithms for sparse linear systems." *ITOR*, vol. 16, no. 4, pp. 465–479, 2009.

(a) Original image

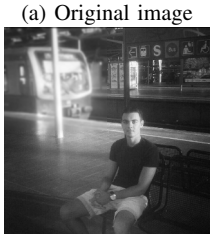

(b) Left top region blurred image

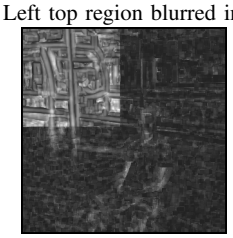

(c) Rough blur map of the blurred image

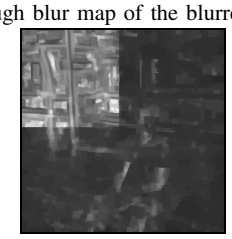

(d) Refined blur map of the blurred image

Fig. 8: Original (a), left top quadrant blurred image (b), rough (c) and refined blur maps (d) where $w_x = 7$, $\beta = 2$ as in the original work

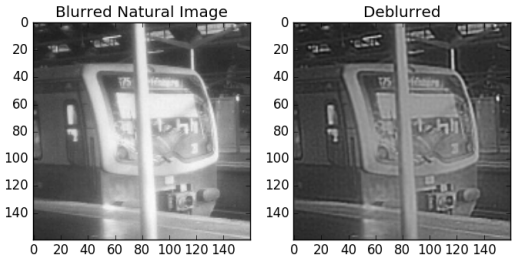

Fig. 9: Own implementation result on a natural image using the method in the paper with gradient descent optimization used instead of primal-dual algorithm for optimization